Measurement of higher-order harmonic azimuthal anisotropy in PbPb collisions at $\sqrt{s_{NN}} = 2.76$ TeV

Content

- Introduction
- CMS Detector
- Event and Track Reconstruction
- Glauber Model Eccentricity
- Methods
- Results
- Summary

Introduction

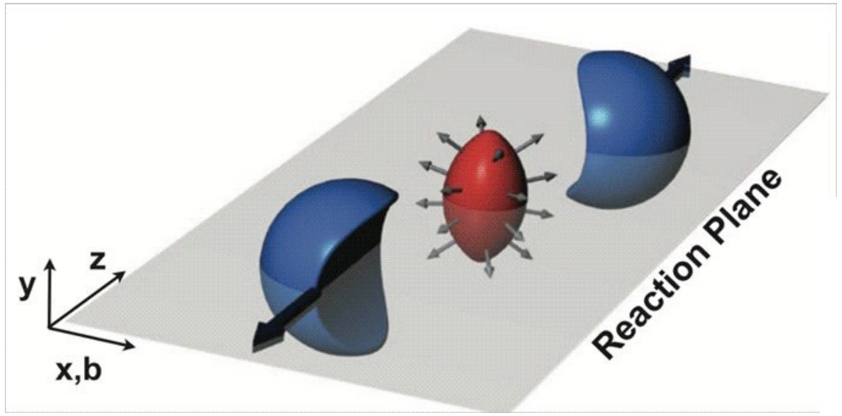

$$\frac{dN}{d\phi} \propto 1 + 2v_2\cos 2(\phi - \Psi_2) + 2v_3\cos 3(\phi - \Psi_3) + 2v_4\cos 4(\phi - \Psi_4)$$

- Anisotropic momentum distribution
- Quark Gluon Plasma (QGP) in local thermal equilibrium
- Anisotropy of event should carry the characteristics and the initial condition of QGP
- This then should reveal hydrodynamics and model of QGP.

https://phys.org/news/2018-10-early-universe-fluid-quark-gluon-plasma.htm

Introduction

- CMS Pb-Pb collision data
- Three methods to measure the different order anisotropic flow with respect to centrality, momentum and eccentricity.
  - **Event-plane**
  - **Cumulant**
  - **Lee-Yang Zero**

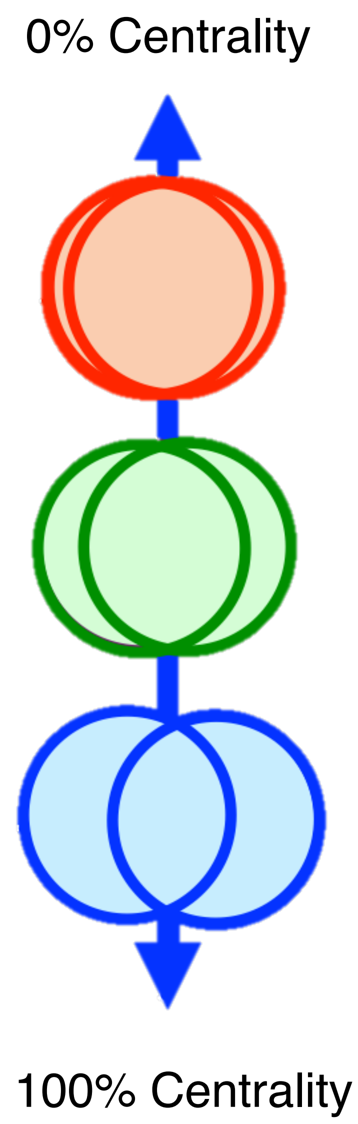

CMS Detector

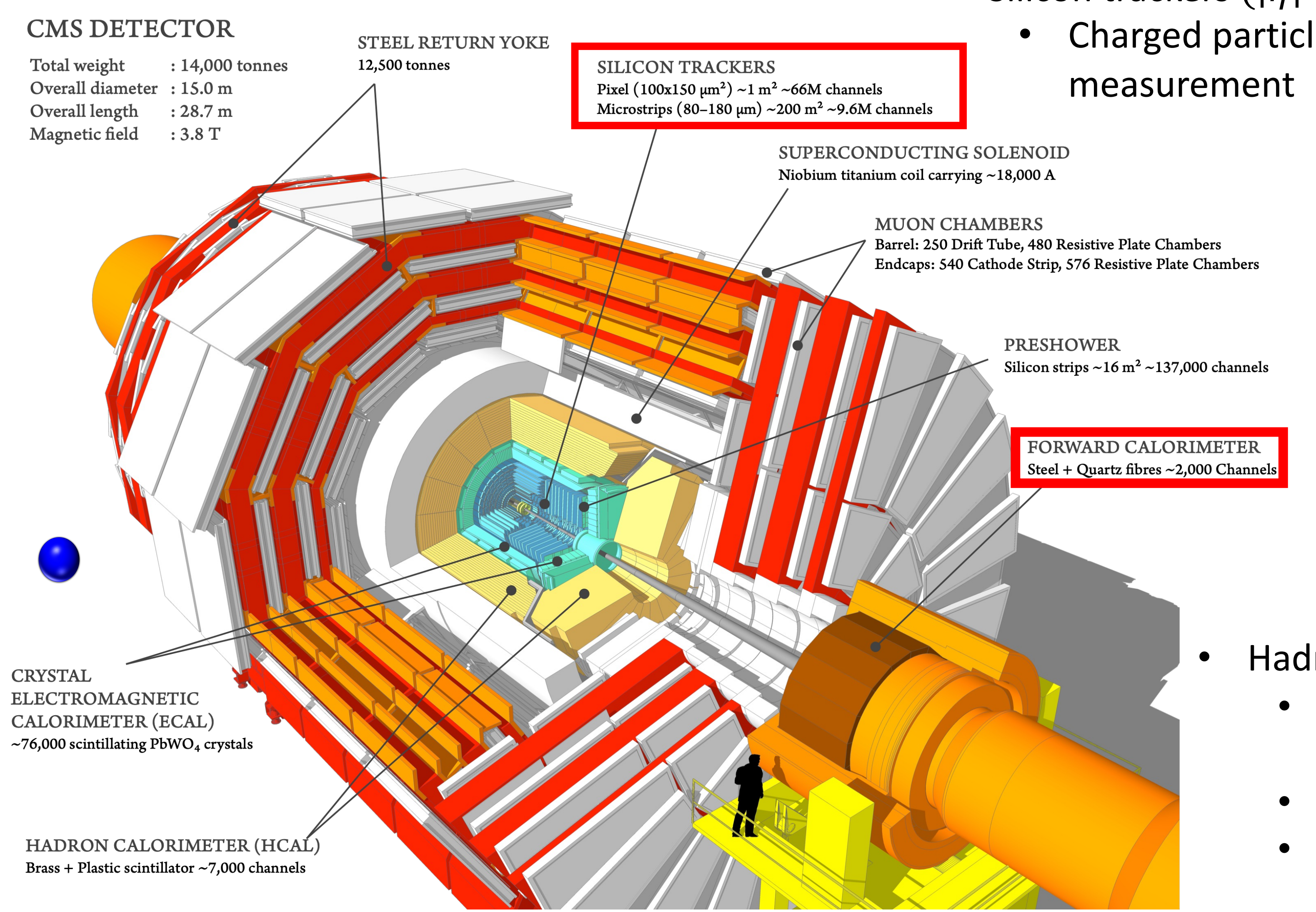

- Silicon trackers ($|\eta| < 2.4$)
  - Charged particles from track reconstruction for anisotropy measurement

- Hadron Forward (HF) Calorimeter ($2.9 < |\eta| < 5.2$)
  - Segmented into $(\phi, \eta) = (0.175\,, 0.175)$ "tower"
  - Used for trigger and beam halo rejection
  - **Reference for event-plane angle**

https://cms-opendata-workshop.github.io/workshop2023-lesson-cms-detector/aio/index.html

Event and Track Reconstruction

- Events triggered by HF coincidence
- 10cm from nominal interaction point
- Remove Ultraperipheral events
  - Three towers in HF with at least $3\ GeV$ energy deposit.
  - Vertex reconstruction
  - Cluster shape from primary vertex
- 22.6×10^{6} events = $3\mu b^{-1}$

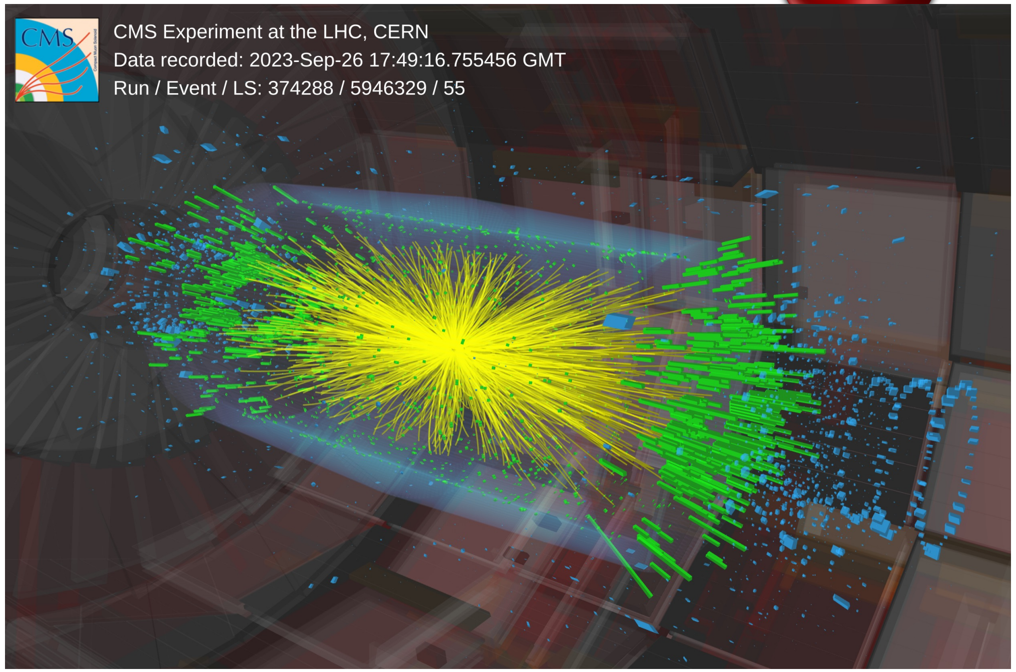

https://cds.cern.ch/record/2872371

Glauber Model Eccentricity

- Nucleon density described by Woods-Saxon density
  - $\rho(r) = \frac{\rho_0(1+\frac{wr^2}{R^2})}{1+e^{\frac{r-R}{a}}}$
- A sequence of independent nucleon-nucleon collisions.
  - Simulate spatial eccentricity
  - $\epsilon_{n,m} = \frac{\sqrt{\langle r_\perp^n \cos[n(\phi-\Phi_m)]\rangle^2}}{\langle r_\perp^n\rangle}, \Phi_\mathrm{m} = \frac{1}{\mathrm{m}}\tan^{-1}\left\{\frac{\langle r_\perp^m \sin[m\phi]\rangle}{\langle r_\perp^m \cos[m\phi]\rangle}\right\}$

Methods (Event-Plane)

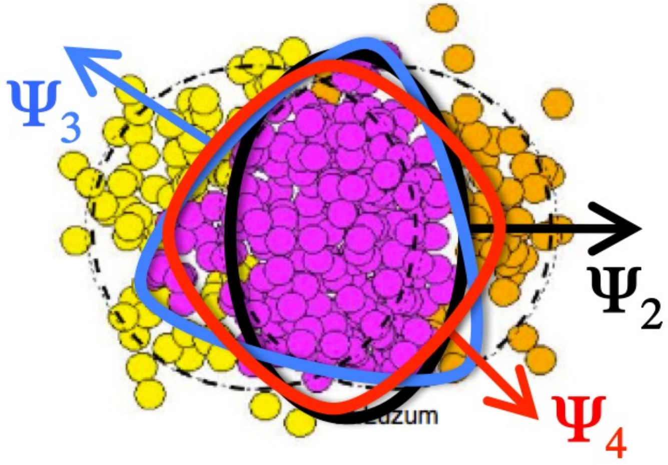

- Sum over HF tower weighted by energy deposit.
  - Approximating $\Psi_m^{\pm} = \frac{1}{m}\tan^{-1}\left\{\frac{\omega_{\mathrm{i}}\sin(m\phi_i)}{\omega_i\cos(m\phi_i)}\right\}$

- In central region $|\eta| < 0.8$, we can measure anisotropy of order n
  - $v_n^{obs}(p_T, \eta) = \ll \cos\left[n\left(\phi - \Psi_m^{\pm}\right)\right] \gg$
    - (≪≫ indicates average over all particles over all events)

- For small p_T, misconstruction of charged particle ≅ 5-25%
  - Require correction using a separate reference angle based on charged track.

Methods (Cumulant & Lee-Yang Zero)

- Generating functions – correlation among particles
  - Adding over all particle correlation gives cumulant
- Reference flow & Differential flow
  - Reference flow averages over broad range of $|\eta| < 0.8$, $p_T < 12$ GeV
  - Differential flow measured with respect to reference flow particles
    - Divided into p_T bins
    - Particle from narrow bin, rest from reference region
- Lee-Yang Zero
  - LYZ accounts for all non-flow contributions that would be neglected in the other methods
  - asymptotic behavior of the cumulant expansion (infinite particle correlation)
  - 2,4,6 order measured reference to 2^{nd} order reference flow

Results

- (Left) Second order anisotropy
  highly depends on the centrality

- (Right) Higher order terms no effected by geometry of QGP, rather shows flat distribution

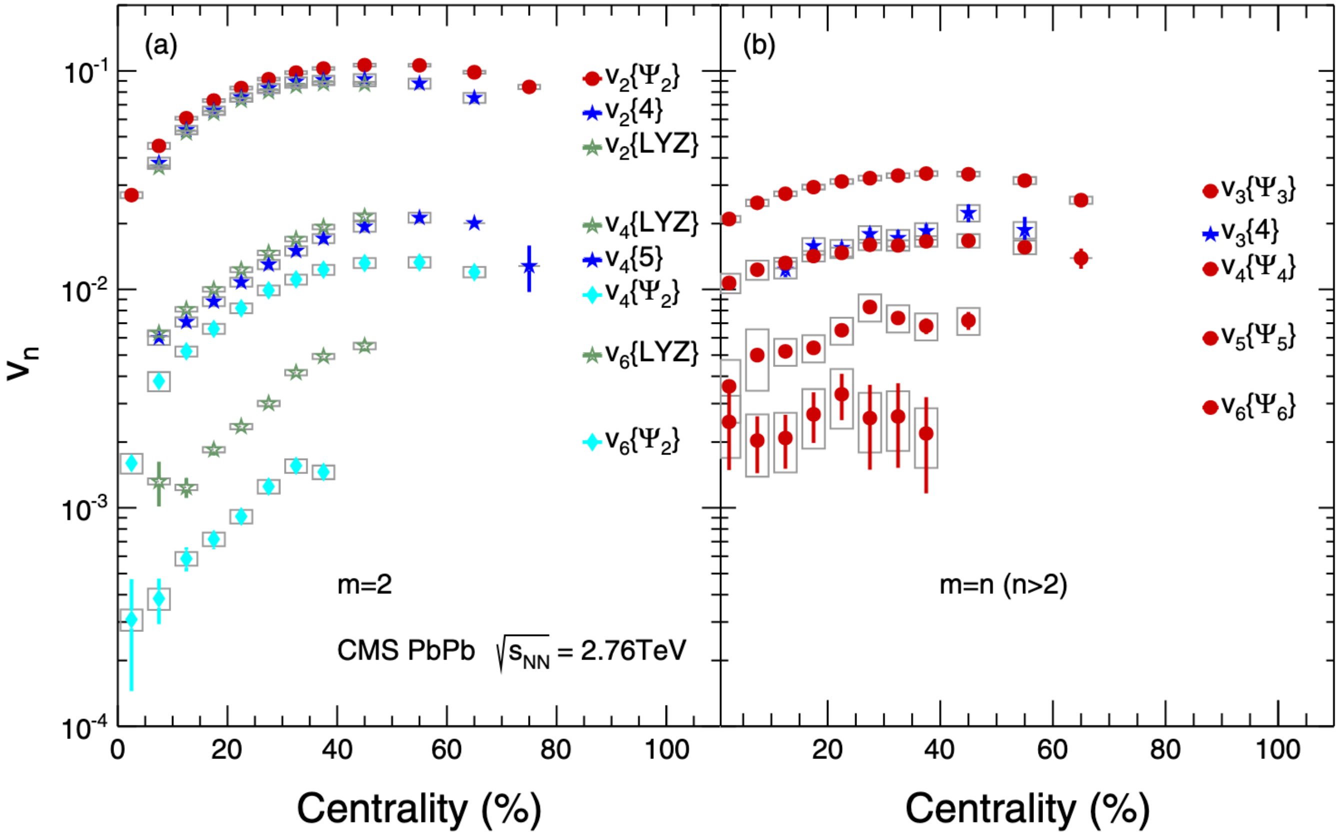

Results

- Eccentricity vs anisotropy
- Linear response at low ϵ
- Large ϵ → smaller QGP
    - Not enough time for particle to interact with QGP

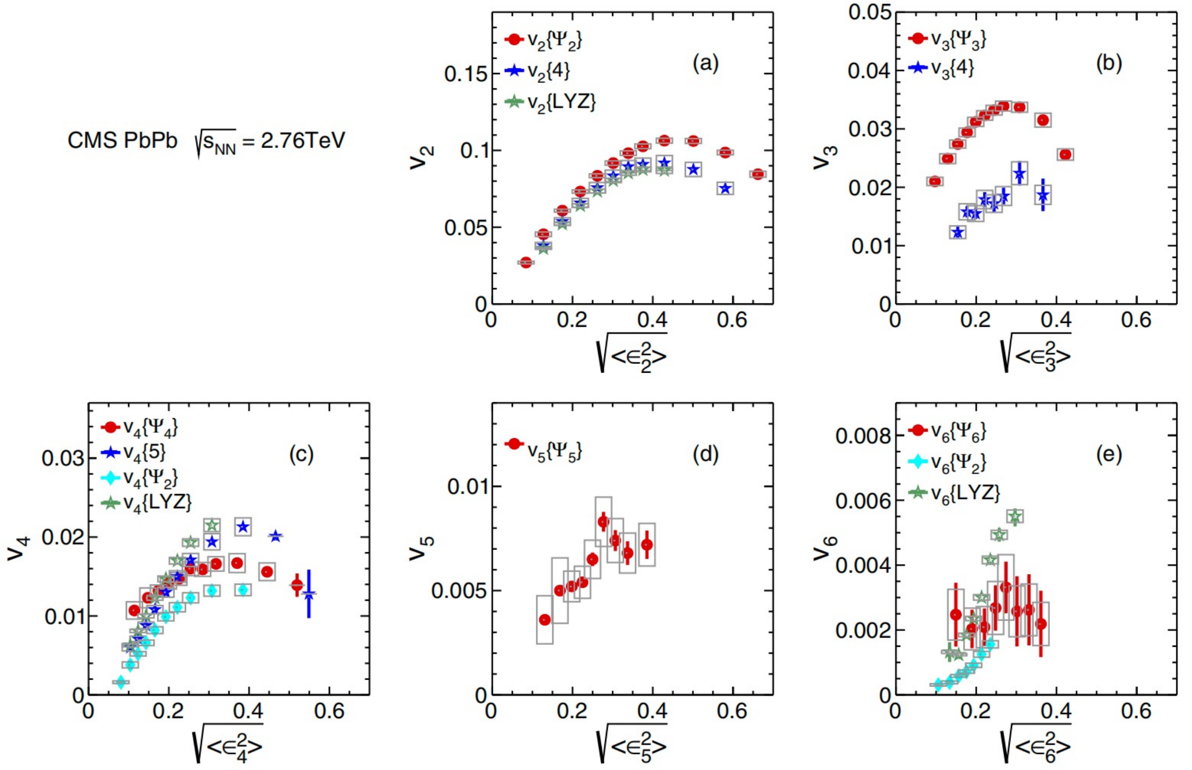

Results

v_3 vs p_T

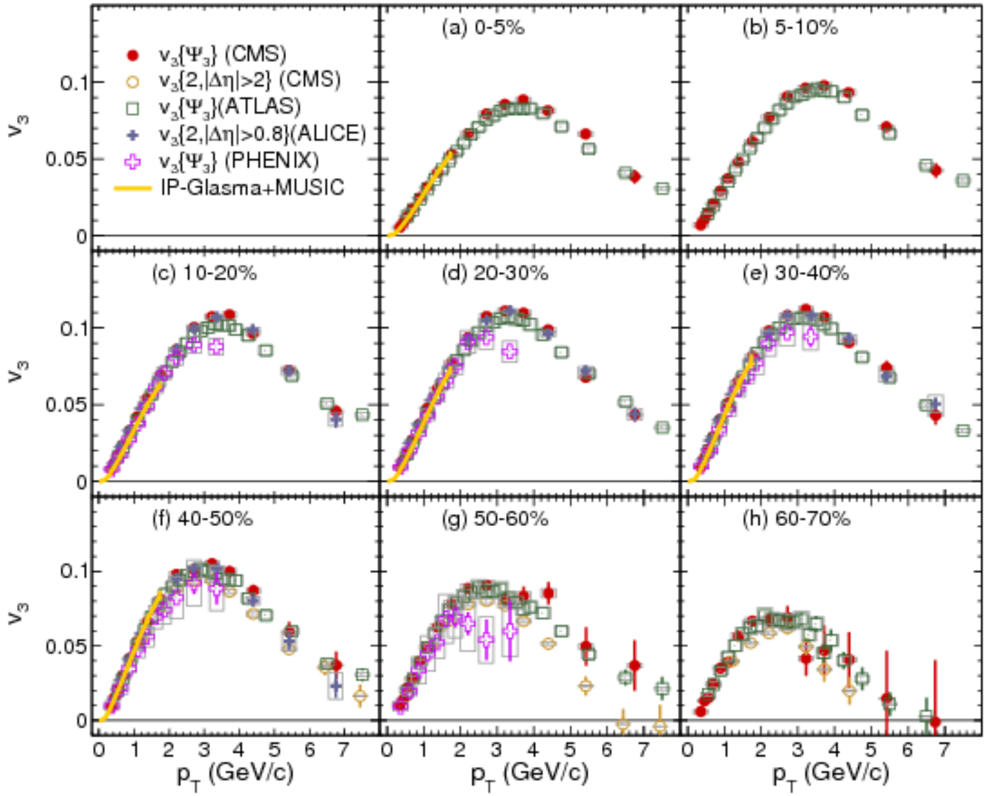

v_5 vs p_T

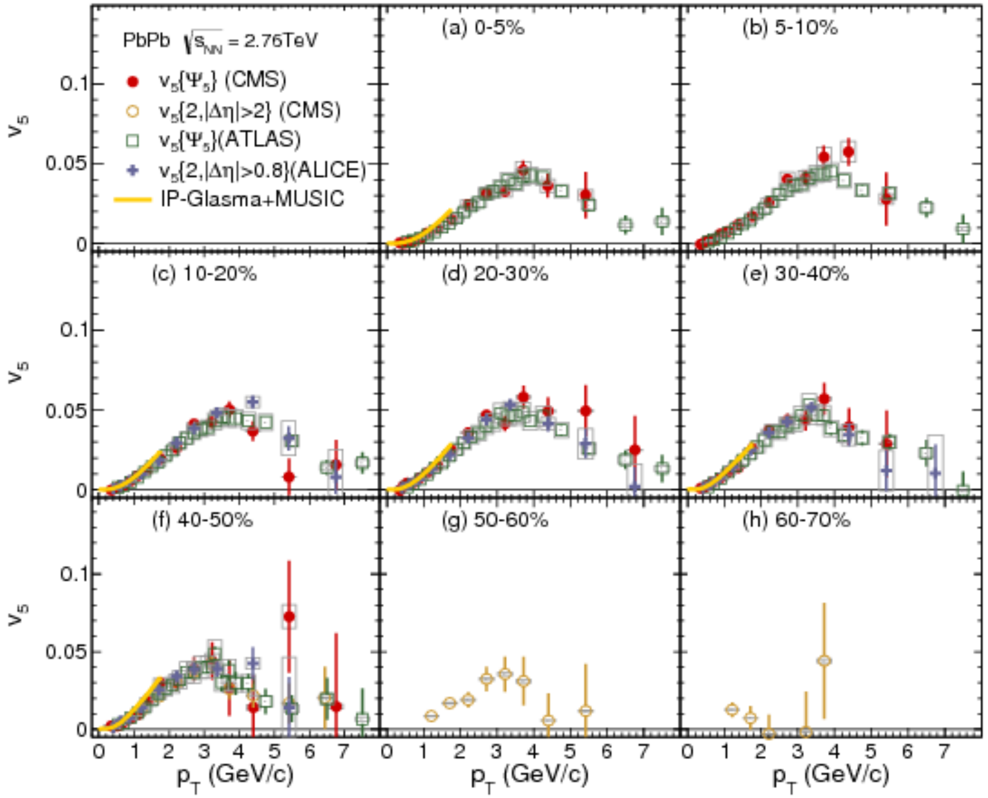

CMS, ATLAS, ALICE, PHENIX and IP-Glasma + MUSIC model

Summary

- High order anisotropy should carry QGP information
  - Initial condition, viscosity, speed of sound, fluctuation
- Using three different method, the higher order anisotropies were measured
- Furthermore, results of second order measurement compared among different methods and experiments
- Many model assumptions of QGP seems to agree with the data.

Back up

Methods (Cumulant & Lee-Yang Zero)

- Generating functions – correlation among particles
  - $G_n(j,k) = \left\langle \prod_{m=1}^{M} \left(1 + r_0 \sqrt{j} e^{i\left(\frac{2\pi k}{8} + \frac{n\phi_m}{M}\right)}\right) \right\rangle$
  - j=1,2,3, k=1,2,…,7, two(three) r_0 for reference (differential) flow
- Cumulant → reference flow (overall) & differential flow (narrow)
  - $v_n\{m\} = \sqrt[m]{-c_n\{m\}}$
  - Differential flow measured with respect to reference flow
    - One particle from narrow bin, rest from reference region

Methods (Lee-Yang Zero)

- Lee-Yang Zero
  - Similar to generating function
  - $g^{\theta}(ir) = \prod_{j=1}^{M}(1 + ir\omega_j \cos(n(\phi_j - \theta)))$
  - The minimum of such function found for 5 θ values
  - Integrated flow estimated as $V_n^{\theta} = \frac{j_{01}}{r_0^{\theta}}$ (j_{01}: First zero of Bessel function J_0)
  - With this integrated flow, differential flow estimated by
    - $\frac{v'_{mn}}{V_n^{\theta}} = \frac{J_1(j_{01})}{J_m(j_{01})} Re\left(\frac{\left\langle g^{\theta}(ir_0^{\theta})\frac{\cos(mn(\psi-\theta))}{1+ir_0^{\theta}\omega_{\psi}\cos(n(\psi-\theta))}\right\rangle_{\psi}}{i^{m-1}\left\langle g^{\theta}(ir_0^{\theta})\sum_j \frac{\cos\left(mn\left(\phi_j-\theta\right)\right)}{1+ir_0^{\theta}\omega_j\cos\left(n\left(\phi_j-\theta\right)\right)}\right\rangle_{events}}\right)$

Event-Based Systematics

- Different hadrons can have different v_n values and tracking efficiency affecting the unidentified, charged-particle results.
- v_n sensitivity to centrality calibration by trigger efficiency scale ±3%.
- HF+ and HF– resolution difference correction. (Significant in high order)
- Various track quality requirements (pointing back to vertex, goodness-of-fit…).

TABLE III. Systematic uncertainties in the $v_3\{\Psi_3\}$ values as a function of centrality in percent. Common uncertainties are shown at the top of the table, followed by those specific to the differential (p_T-dependent) and integral ($|\eta|$-dependent) measurements.

Source		Centrality		
		0%–10%	10%–50%	50%–70%
Particle composition		0.5	0.5	0.5
Centrality determination		1.0	1.0	1.0
Resolution correction		1.0	1.0	3.0
[Differential]	p_T (GeV/c)			
Track quality requirements	0.3–0.4	20	10	20
	0.4–0.8	3.0	2.0	2.0
	0.8–8.0	1.0	1.0	1.0
Total (p_T)	0.3–0.4	20	10	20
	0.4–0.8	3.4	2.5	3.8
	0.8–8.0	1.8	1.8	3.4
[Integral]	$\|\eta\|$			
Track quality requirements	0.0–1.6	3.0	2.0	2.0
	1.6–2.4	6.0	4.0	4.0
Total ($\|\eta\|$)	0.0–1.6	3.4	2.5	3.8
	1.6–2.4	6.2	4.3	5.1

Cumulant and LYZ Systematics

TABLE X. Systematic uncertainties in the $v_4\{5\}$ values as a function of centrality in percent. Common uncertainties are shown at the top of the table, followed by those specific to the differential (p_T-dependent) and integral ($|\eta|$-dependent) measurements.

Source		Centrality		
		5%–10%	10%–40%	40%–60%
Particle composition		0.5	0.5	0.5
Centrality determination		1.0	1.0	1.0
Multiplicity fluctuations		1.0	2.0	3.0
r_0(%)		5.0	3.0	3.0
[Differential]	p_T (GeV/c)			
Track quality requirements	0.3–0.5	15	5.0	5.0
	0.5–0.8	10	3.0	3.0
	0.8–8.0	5.0	1.0	1.0
Total (p_T)	0.3–0.5	16	6.3	6.7
	0.5–0.8	11	4.8	5.3
	0.8–8.0	7.2	3.9	4.5
[Integral]	$\|\eta\|$			
Track quality requirements	0.0–0.8	5.0	3.0	3.0
Total ($\|\eta\|$)	0.0–0.8	7.2	4.8	5.3

TABLE XII. Systematic uncertainties in the $v_6\{\mathrm{LYZ}\}$ values as a function of centrality in percent. Common uncertainties are shown at the top of the table, followed by those specific to the differential (p_T-dependent) and integral ($|\eta|$-dependent) measurements.

Source		Centrality		
		5%–10%	10%–40%	40%–60%
Particle composition		0.5	0.5	0.5
Centrality determination		1.0	1.0	1.0
Multiplicity fluctuations		0.1	0.9	2.0
[Differential]	p_T (GeV/c)			
Track quality requirements	0.3–0.5	16	12	7.5
	0.5–8.0	6.0	4.0	3.0
Total (p_T)	0.3–0.5	16	13	7.8
	0.5–8.0	6.1	4.2	3.8
[Integral]	$\|\eta\|$			
Track quality requirements	0.0–0.8	3.0	2.5	3.5
Total ($\|\eta\|$)	0.0–0.8	3.2	2.9	4.2

Different r_0 parameter
results with and without the selection of 80% of the mean multiplicity.

Heavy Ion Model

- Glauber model
  - Collision model

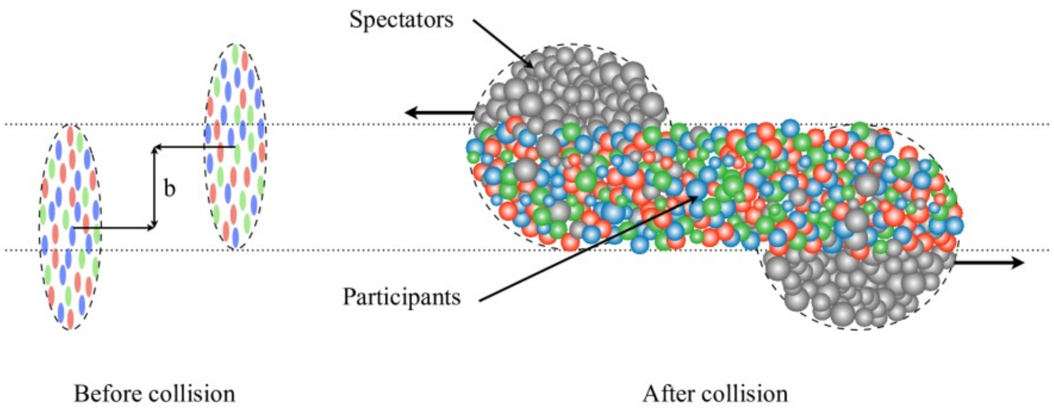

- the nucleus-nucleus interaction in terms of elementary nucleon-nucleon interaction
- It assumes
  - The nuclei follow a straight-line trajectory
  - The nucleons as a point-like object

- Color Glass Condensate (CGC) model
  - Nucleus model before collision

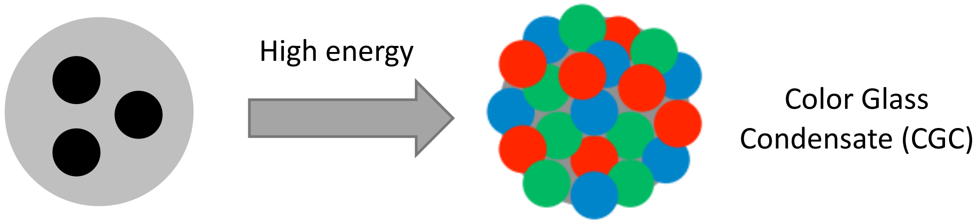

- Dense gluonic states in hadrons which universally appear in the high-energy limit of scattering
  - When the density of gluons becomes high, they start to interact with each other → CGC
- Fluctuations of a fast moving parton become real particles in reactions

The anisotropy also depends on the initial conditions,
whether the Glauber-like picture prevails or if gluon-saturated effects, as found in the CGC model

Heavy Ion Model

- With this experiment, it cannot be determined which nuclear model describes the collision better.

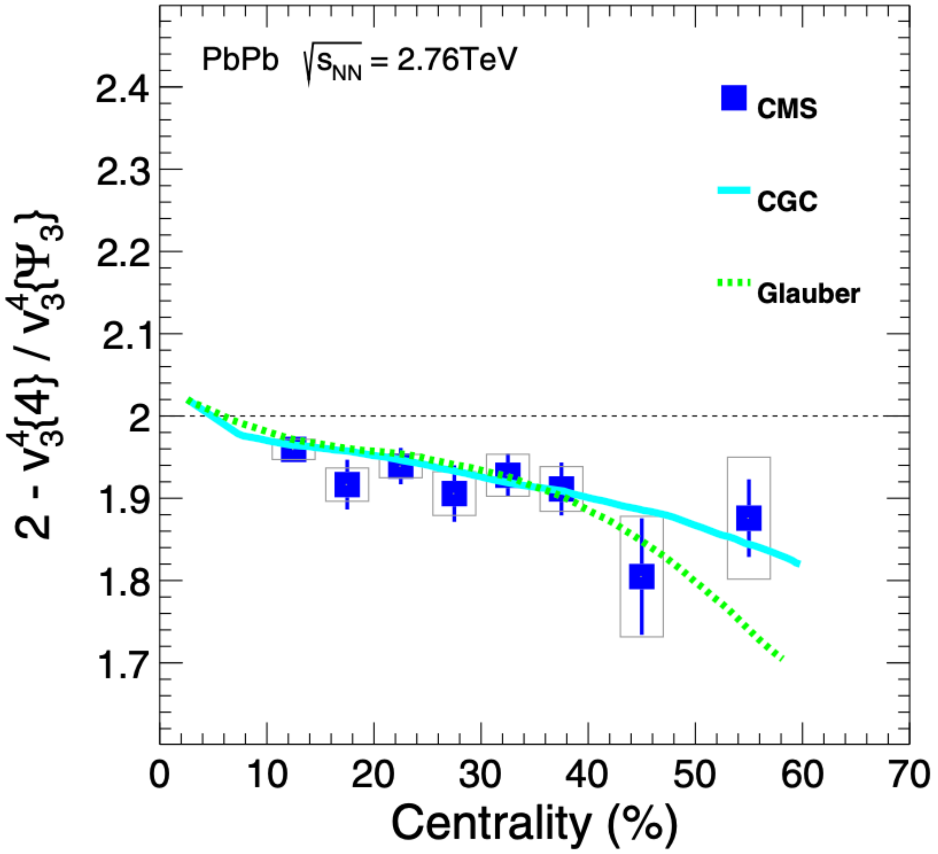

Additional back up

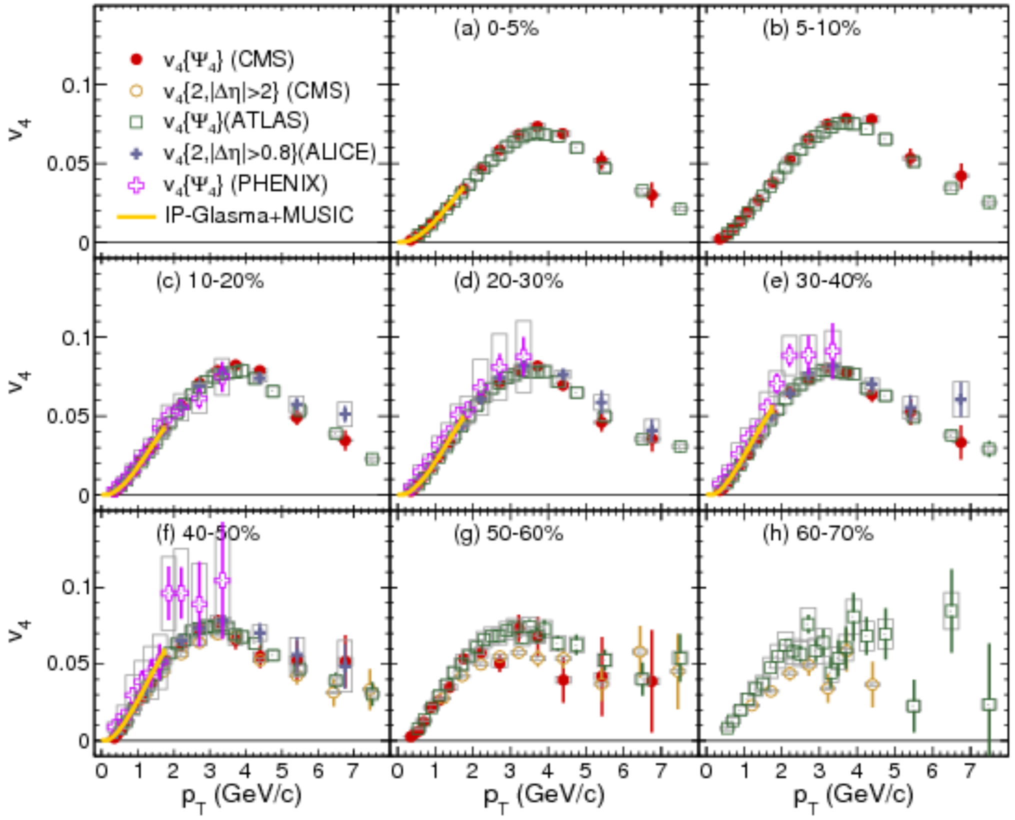

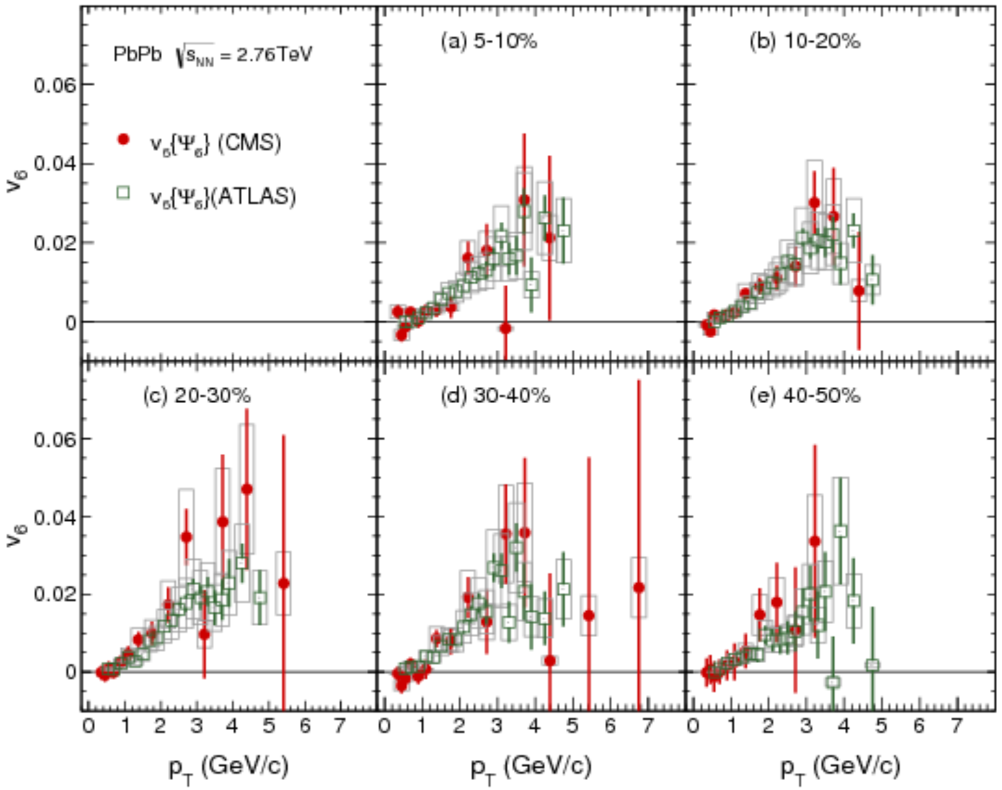

Comparison of the v_4 (left, fig 10) and v_6 (right, fig 12) results of CMS, ATLAS, ALICE, PHENIX and IP-Glasma + MUSIC model